

Vibration damping in gantry crane systems: Finite horizon optimal control approach

Martin Gubej
NTIS Research Centre
University of West Bohemia
Pilsen, Czech Republic
mgubej@ntis.zcu.cz

Václav Helma
NTIS Research Centre
University of West Bohemia
Pilsen, Czech Republic
helma@ntis.zcu.cz

Abstract—The paper deals with the problem of anti-sway control in human-operated gantry cranes. The goal is to design a suitable algorithm aiming at minimization of unwanted transient and residual oscillations of the manipulated load. A finite horizon optimization is adopted for the derivation of an optimal open-loop control strategy. The novelty of the proposed approach comes from the combination of model-based predictive control and zero-vibration input shaping methods. This allows utilizing some key advantages from both fields in terms of performance, robustness, constraints definition and simplicity of implementation. Experimental case study demonstrates the proposed approach and compares it to conventional input-shaping method.

Index Terms—vibration control, anti-sway control, gantry cranes, optimal control, feedforward control, zero vibration shaper, input shaping, model predictive control

I. INTRODUCTION

Gantry crane systems are used in numerous applications ranging from factory automation to ship-to-shore container terminals or building construction. One of their troublesome properties comes from the inherently oscillatory dynamics caused by the hanging load. Care must be taken when operating the gantry to avoid excessive sway of the load which may cause unwanted collisions or damage of the cargo. Human operated cranes require qualified personnel capable of high accuracy handling.

Several automatic anti-sway control systems are being developed and integrated in the gantry equipment aiming at reduction of the unwanted transient and residual oscillations. The methods of Zero vibration (ZV) input shaping have become one of the favorite approaches to accomplish this task due to simplicity of use, robustness and possibility of operation in an open-loop manner without additional instrumentation. The fundamental idea is to properly modify the trajectory of the gantry in a way that minimizes the level of motion-induced oscillations of the hanging load. The pioneering work in this field was done by Smith [1], followed by further theoretical achievements in 1990s by Singer, Seering and Singhose [2]–[4]. Numerous design methods emerged later [5]–[10] with several successful applications in crane control [11], [12]. Other proposed approaches involve input-output inversion techniques [13], model-predictive control (MPC) [14] or convex optimization [15]. An extensive survey of crane control methods is given in [16].

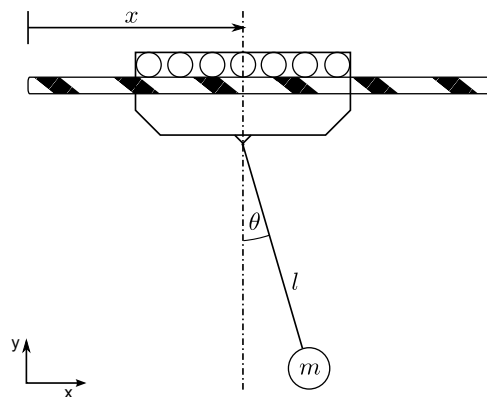


Fig. 1. Gantry crane system in the anti-sway control scenario

One of the drawbacks of the classical input shaping methods comes from their inability to incorporate physical constraints on the generated trajectory directly into the design requirements. This may lead to infeasible motions which cannot be tracked by physical actuators. This problem is addressed directly in MPC allowing to limit plant inputs, states and outputs. On the other hand, MPC with its receding horizon strategy belongs to feedback control strategies requiring additional instrumentation to detect load motion, it comes with much higher computational demands and does not allow to directly include robustness requirements as in the case of ZV shapers.

The main motivation was to connect the two fields of optimal control and ZV input shaping and develop a design algorithm which combines the best of both realms in terms of robustness, simplicity and direct specification of actuator/plant constraints. Section II formulates the considered anti-sway control problem. Section III presents some fundamental ideas from the ZV input shaping theory. Section IV comes with the novel optimal design method which is experimentally validated by means of a small-scale gantry system model, as shown in Section V.

II. GANTRY CRANE MODEL

One axis of a portal crane system shown in Fig. 1 is considered for the anti-sway control scenario. The goal is to manipulate the overhead gantry based on the human operator

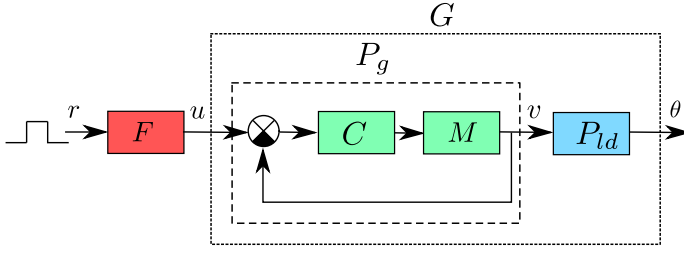


Fig. 2. **Assumed control structure:** r - velocity setpoint reference set by a human operator, F - reference shaping filter, P_g - gantry subsystem containing the internal velocity loop, C - velocity controller, M - gantry+drive dynamics, P_{ld} - load side dynamics, G - overall plant

commands while minimizing unwanted oscillations of the hanging load.

A single-link pendulum model of the plant dynamics is used for simplicity. However, multiple oscillatory modes can be considered without loss of generality. The gantry is typically equipped by a drive with a closed velocity control loop. It is assumed that the closed-loop bandwidth is high enough to attenuate potential disturbances generated by reaction forces coming from the hanging load. The equation of motion can be derived using the Lagrange formalism or Newton-Euler equations in the form of

$$\ddot{\theta} + \frac{b}{ml^2}\dot{\theta} + \frac{g}{l}\sin(\theta) = -\frac{1}{l}\ddot{x}\cos(\theta), \quad (1)$$

where θ denotes the load sway angle, x is gantry position and m, l, b are the parameters of load mass, rope length and damping. For small declination angles of the load around the stable equilibrium $\theta \approx 0$, it holds that $\sin(\theta) \approx \theta$, $\cos(\theta) \approx 1$ and the equation (1) reduces to a linear system approximation:

$$\ddot{\theta} + \frac{b}{ml^2}\dot{\theta} + \frac{g}{l}\theta = -\frac{1}{l}\ddot{x}. \quad (2)$$

Assuming a crane system with an internal velocity control loop and applying the Laplace transform to (2), we obtain the transfer function from the gantry speed to the load sway as:

$$P_{ld}(s) = \frac{\theta(s)}{\dot{x}(s)} = -\frac{\frac{1}{l}s}{s^2 + \frac{b}{ml^2}s + \frac{g}{l}} \triangleq \frac{Ks}{s^2 + 2\xi\omega_n s + \omega_n^2};$$

$$\omega_n = \sqrt{\frac{g}{l}}, \quad \xi = \frac{b}{2m\sqrt{gl^3}}, \quad K = -\frac{1}{l}. \quad (3)$$

A discrete-time equivalent suitable for sampled-data control synthesis can be derived by applying bilinear Tustin transform

$$P_{ld}(z) = \frac{\theta(z)}{V(z)} = P(s)\Big|_{s=\frac{2(z-1)}{T(z+1)}}, \quad (4)$$

where $P_{ld}(z)$ is the discrete transfer function defined in the Z-transform for a given sampling period T , $V(z) = \mathcal{Z}\{v(kT)\}$; $v(kT) = \dot{x}(kT)$ is the actual gantry velocity and $\theta(z) = \mathcal{Z}\{\theta(kT)\}$ is the load sway angle.

The velocity loop dynamics of the gantry drive is assumed in the form of transfer function

$$P_g(z) = \frac{V(z)}{U(z)} = \frac{b_1z + b_0}{z^2 + a_1z + a_0}z^{-d}, \quad (5)$$

where $U(z) = \mathcal{Z}\{u(kT)\}$ denotes the setpoint value of the drive velocity controller. This is a generic form suitable for a wide range of industrial crane systems when considering rigid body dynamics of the gantry and a PI controller in the velocity loop. The delay term models potential communication lag between the drive and a supervisory controller. More complex model structures may be introduced when needed.

Under assumption of negligible load to drive disturbances, the overall dynamics of the system becomes

$$G(z) = \frac{\theta(z)}{U(z)} = P_g(z)P_{ld}(z). \quad (6)$$

The reference values r for the desired gantry motion are set by a human operator, typically in the ON-OFF fashion with a given constant jog velocity value. A reference shaping filter F is introduced to alleviate unwanted load oscillations. Overall schematics showing the assumed control structure is shown in Fig. 2. Derivation of the shaping filter $F(z)$ follows in the next sections.

III. CONVENTIONAL INPUT SHAPING

A common approach to design of the input shaper F in case of an oscillatory plant is to employ a class of Zero Vibration (ZV) shaping filters. Their structure usually consists of a set of weighted sum of time-delays

$$F(s) = \frac{U(s)}{R(s)} = \sum_{i=1}^n A_i e^{-t_i s}. \quad (7)$$

The shaper parameters t_i, A_i are commonly designed using the *residual vibration function* (sometimes called *sensitivity function*)

$$V(\omega, \xi) = e^{-\xi\omega t_n} \sqrt{C(\omega, \xi)^2 + S(\omega, \xi)^2}, \quad (8)$$

where

$$C(\omega, \xi) = \sum_{i=1}^n A_i e^{\xi\omega t_i} \cos(\omega\sqrt{1-\xi^2}t_i), \quad (9)$$

$$S(\omega, \xi) = \sum_{i=1}^n A_i e^{\xi\omega t_i} \sin(\omega\sqrt{1-\xi^2}t_i), \quad (10)$$

determining the relative amplitude of the induced residual vibrations at time $t = t_n$ [3], [4] for the flexible mode described by the parameters of natural frequency and damping ω, ξ .

In order to minimize the level of excited oscillations, the Zero Vibration condition

$$V(\omega, \xi) = 0 \rightarrow \sqrt{C(\omega, \xi)^2 + S(\omega, \xi)^2} = 0 \quad (11)$$

must hold giving the necessary condition for the shaper parameters. The residual vibration function (8) also serves for the quantification of shaper robustness to uncertainty in the model parameters ω, ξ . A common way to enhance such robustness at a given mode is to enforce a flat slope of the sensitivity function frequencies by imposing first l derivatives to be zero

$$\frac{\partial^l V(\omega, \xi)}{\partial \omega^l} = 0, \quad \frac{\partial^l V(\omega, \xi)}{\partial \xi^l} = 0. \quad (12)$$

An alternative is to keep the level of vibrations below some defined value using the inequality constraints

$$V(\bar{\omega}_i, \bar{\xi}_k) \leq V^{max}, \quad (13)$$

where $\bar{\omega}_i, \bar{\xi}_k$ denotes a set of points forming a region around the mode ω, ξ which is to be compensated.

The Zero vibration filters were successfully applied in many application domains. Numerous design methods exist allowing to find a suitable trade-off between robustness and delay introduced by the shaper [9]. However, there are some fundamental disadvantages which may prevent them to be used effectively in crane motion control systems:

- 1) **Standard design methods do not allow formulation of constraints on the generated motion profiles**, the shaper may work in certain regimes but fail by hitting the plant physical limits e.g. in higher speed regions thanks to its structure of linear filter, the actuator resources are not effectively used
- 2) **The finite transient time** which is often presented as one of important benefits holds only for the oscillatory modes of the system, there is no guarantee giving a final transient time for the rest of the plant dynamics

The proposed novel design methodology tries to overcome the mentioned drawbacks of the ZV shapers while preserving their key advantages in terms of performance and robustness.

IV. FINITE HORIZON OPTIMAL CONTROL

The starting point is an arbitrary state-space form of the overall plant G including both load and gantry dynamics (6) without the delay term which does not affect the final solution:

$$\begin{aligned} \mathbf{x}(k+1) &= \mathbf{A}\mathbf{x}(k) + \mathbf{B}u(k), \\ \mathbf{z}(k) &= [\theta(k), v(k), a(k), j(k)]^T = \mathbf{C}\mathbf{x}(k), \end{aligned} \quad (14)$$

where the vector \mathbf{z} contains the penalized outputs defined as the sway angle θ , gantry velocity v , acceleration a and jerk j . The last two outputs can be defined in terms of numerical differentiation

$$a(k) = \frac{v(k) - v(k-1)}{T}, \quad j(k) = \frac{a(k) - a(k-1)}{T}. \quad (15)$$

There always exists a finite time sequence of inputs

$$\mathbf{u} \triangleq [u(0), u(1), \dots, u(n-1)]^T \quad (16)$$

which allows a transfer from an arbitrary initial state $\mathbf{x}_0 = \mathbf{x}(0)$ to an arbitrary final state $\mathbf{x}_f = \mathbf{x}(n)$ in a finite number of n steps, provided that $n \geq o$, where $o = \dim(\mathbf{x})$ is the order of the system and the pair $\{\mathbf{A}, \mathbf{B}\}$ is reachable.

The system can stay in the new state \mathbf{x}_f for an arbitrary long time if and only if it belongs to the set of plant equilibrium states and correct constant input is applied for $k \geq n$. The crane dynamics contains an infinite number of equilibrium states corresponding to an arbitrary constant velocity of the drive $v(k) = \text{const.}$ and the load hanging in the lower stable position $\theta(k) = 0$ with zero angular velocity $\dot{\theta}(k) = 0$.

There is a unique solution for the time-optimal input sequence in the limit case $n = o$ given as

$$\bar{\mathbf{u}} = \mathbf{Q}_r^{-1}(\mathbf{x}_f - \mathbf{A}^n \mathbf{x}_0), \quad (17)$$

where $\mathbf{Q}_r \triangleq [\mathbf{B}, \mathbf{A}\mathbf{B}, \dots, \mathbf{A}^{n-1}\mathbf{B}]$ is the (regular) reachability matrix of the system and $\bar{\mathbf{u}}$ is the input sequence vector (16) in the reversed order of the input samples.

Such result is seldom applicable in practice as it typically produces excessive control inputs and there are no additional degrees of freedom allowing to formulate any complementary design requirements.

On the other hand, an infinite number of solutions exist for the case $n > o$. This allows to include some additional constraints on system inputs, states or outputs, define a suitable cost function and select one particular optimal solution.

The most important requirements to be considered for the crane control scenario are as follows:

- **Maximum velocity** - given by the motor and drive system propelling the gantry
- **Maximum acceleration** - given by the maximum torque/force the motor can produce
- **Maximum jerk** - allows to enforce smooth motion commands to avoid excitation of unmodelled dynamics, improves energy efficiency and lowers mechanical wear
- **Maximum load sway angle** - to guarantee safe manipulation with the hanging load

Time evolution of the mentioned physical quantities can be expressed from the general solution of the state and output equation in (14)

$$\mathbf{z}(k) = \mathbf{C}\mathbf{A}^k \mathbf{x}(0) + \mathbf{C} \left[\mathbf{A}^{(k-1)}\mathbf{B}, \dots, \mathbf{A}\mathbf{B}, \mathbf{B} \right] \mathbf{u} \quad (18)$$

The important physical plant/actuator constraints can be expressed as

$$|z_i(k)| \leq z_i^{max} \quad \forall k = 1..n, i = 1, \dots, 4, \quad (19)$$

$$u_{min} \leq u(k) \leq u_{max}, \quad \forall k = 0, \dots, n-1, \quad (20)$$

$$a(k) \geq 0 \text{ or } a(k) \leq 0, \quad \forall k, \quad (21)$$

giving maximum absolute value bounds, limits for the generated setpoint sequence and condition of monotonous response. All of them can be translated into the inequality constraints:

$$\mathbf{A}_{ineq} \mathbf{u} \leq \mathbf{B}_{ineq}. \quad (22)$$

A quadratic cost function penalizing the transient maneuver can be chosen as:

$$\mathbf{J}(\mathbf{u}) = \sum_{i=0}^{n-1} \mathbf{e}_i^T \mathbf{Q}_i \mathbf{e}_i + r_i u_i^2 \quad (23)$$

where \mathbf{e}_i is a vector of setpoint tracking errors defined as

$$\mathbf{e}_i = \mathbf{w}(i) - \mathbf{z}(i); \quad \mathbf{w}(i) = [0, v_f, 0, 0]^T \quad \forall i, \quad (24)$$

with the constant reference vector \mathbf{w} defining the final equilibrium state at the given constant velocity v_f set by the human operator, $\mathbf{Q}_i \geq 0$ is a positive semi-definite matrix penalizing the individual outputs and $r_i > 0$ penalizes the control input.

The cost function can be rearranged to the form of

$$J(\mathbf{u}) = \frac{1}{2} \mathbf{u}^T \underbrace{(\mathbf{H}^T \mathbf{Q}' \mathbf{H} + \mathbf{R})}_{\triangleq \mathbf{F}} \mathbf{u} + \underbrace{((\mathbf{x}_0^T \mathbf{P}^T - \mathbf{w}^T) \mathbf{Q}')}_{\triangleq \mathbf{g}^T} \mathbf{H} \mathbf{u}, \quad (25)$$

where $\mathbf{Q}' \in \mathbb{R}^{4n \times 4n}$ is a block-diagonal matrix consisting of the \mathbf{Q}_i matrices, $\mathbf{R} \in \mathbb{R}^{n \times n}$ is a diagonal matrix containing the r_i terms and \mathbf{H}, \mathbf{P} are the prediction matrices defined as

$$\mathbf{P} \triangleq [\mathbf{C} \quad \mathbf{C}\mathbf{A} \quad \mathbf{C}\mathbf{A}^2 \quad \dots \quad \mathbf{C}\mathbf{A}^{n-1}]^T, \quad (26)$$

$$\mathbf{H} \triangleq \begin{bmatrix} \mathbf{0} & \mathbf{0} & \mathbf{0} & \dots \\ \mathbf{C}\mathbf{B} & \mathbf{0} & \mathbf{0} & \dots \\ \mathbf{C}\mathbf{A}\mathbf{B} & \mathbf{C}\mathbf{B} & \mathbf{0} & \dots \\ \mathbf{C}\mathbf{A}^2\mathbf{B} & \mathbf{C}\mathbf{A}\mathbf{B} & \mathbf{C}\mathbf{B} & \vdots \\ \mathbf{C}\mathbf{A}^{n-2}\mathbf{B} & \mathbf{C}\mathbf{A}^{n-3}\mathbf{B} & \mathbf{C}\mathbf{A}^{n-4}\mathbf{B} & \dots \end{bmatrix}.$$

The optimal solution can be found by minimizing the cost function

$$\mathbf{u}^* = \underset{\forall \mathbf{u}}{\operatorname{argmin}} \{J(\mathbf{u}) = \frac{1}{2} \mathbf{u}^T \mathbf{F} \mathbf{u} + \mathbf{g}^T \mathbf{u}\} \quad (27)$$

$$\text{w.r.t. } \mathbf{A}_{eq} \mathbf{u} = \mathbf{B}_{eq}, \mathbf{A}_{ineq} \mathbf{u} \leq \mathbf{B}_{eq}, \mathbf{u}_{min} \leq \mathbf{u} \leq \mathbf{u}_{max}, \quad (28)$$

which is a standard quadratic programming problem. There is one globally optimal solution due to the positive definiteness of \mathbf{F} which follows from its construction provided that the formulated constraints lead to a non-empty set of feasible solutions.

The problem formulation corresponds to the standard linear model predictive control (MPC) up to this point for a special case of identical prediction and control horizon. The main difference is that the MPC approach adopts a receding horizon strategy which repeats the optimization at each sampling instants and applies only the first input. In our approach, the **optimization is performed off-line only once** and the resulting optimal sequence is stored in the target control platform, ready to be used in the open-loop manner once the operator command arrives.

The second difference comes from the constraint on reaching the *new equilibrium state* at the last time instant, i.e.

$$\mathbf{x}(k) = \mathbf{x}_f, \mathbf{z}(k) = \mathbf{w} \quad \forall k \geq n, \quad (29)$$

which is not normally used in MPC and which adds another equality constraints in the quadratic optimization problem (28). This allows to achieve a **finite settling time for the whole plant**, not only the flexible modes as in the case of conventional ZV shapers.

The last difference is in the introduction of **robustness to modelling errors** which is normally not covered in the standard MPC problem formulation.

Proposition 1. *The robustness to uncertainty in plant parameters ω, ξ can be achieved analogously to the standard ZV shaper design methods via the sensitivity function constraints (12,13) assuming a discrete FIR filter structure*

$$F(z) = \frac{U(z)}{R(z)} = \sum_{i=1}^n A_i z^{-(i-1)}, \quad (30)$$

and its impulse response coefficients related to the optimal input sequence \mathbf{u}^* in (27) as follows

$$A_1 = u^*(0), \quad A_i = \Delta u^*(i-1) = u^*(i-1) - u^*(i-2), \quad i = 2, \dots, n \quad (31)$$

Proof. The filter F from Fig. 2 constructed according to (30,31) with a dummy constant reference signal $r(k) = 1 \forall k$ generates the shaped input sequence

$$u(k) = \sum_{i=1}^{k+1} A_i, \quad (32)$$

which is equivalent to the optimal solution \mathbf{u}^* obtained from the quadratic optimization. Therefore, additional equality or inequality constraints in (28) can be used to enforce the robustness via residual vibration function shaping as in the case of robust ZV shapers. \square

Time-optimal trajectory can be derived by forming a modified optimization problem

$$\mathbf{u}_t^* = \underset{\forall n}{\min}(n) \{ \underset{\forall \mathbf{u}}{\operatorname{argmin}} \{J(\mathbf{u}) = \frac{1}{2} \mathbf{u}^T \mathbf{F} \mathbf{u} + \mathbf{g}^T \mathbf{u}\} \}. \quad (33)$$

which searches for the minimum achievable length n for which a feasible solution exists.

Algorithm 1 Finite horizon optimal control algorithm

Input: Plant model G , input/state/output constraints (e.g. actuator velocity, acceleration, jerk, load sway...)

Output: Optimal input sequence / equivalent shaping filter F

- 1: Set initial state \mathbf{x}_0 and final equilibrium \mathbf{x}_f
 - 2: Set physical constraints
 - 3: Set transient time n / opt for the time optimal solution
 - 4: (Optional) Formulate robustness conditions via residual vibration function shaping (12,13)
 - 5: Choose cost function weights \mathbf{Q}_i, r_i (23)
 - 6: Solve the QP problem (27) or (33)
 - 7: Store the resulting optimal input \mathbf{u}^* or the equivalent shaping filter F (30,31) in the target real-time platform
 - 8: Apply the precomputed trajectory based on the operator commands
-

V. EXPERIMENTAL RESULTS

A pendulum-cart system (Fig. 3) was used as a small-scale model simulating the gantry crane dynamics. The cart is driven via a toothed belt from a three-phase AC induction motor. Current and velocity loop in the standard PID cascade control scheme is realized by YASKAWA AC Drive-A1000 frequency inverter. The tested input shaping filters are implemented in REXYGEN control system [17] running on Raspberry Pi with Monarco HAT as an input-output interface. Cart position and payload sway angles are measured using incremental encoders. The load angle was not used for feedback control, it serves for the validation purpose only.

The motor dynamics was approximated by the second order model (5) with parameters obtained from frequency response function (FRF) fitting. The FRF data were acquired



Fig. 3. Mechanical system used for the experiments

from the preceding nonparametric identification process based on spectra averaging of periodic signals. The identification procedure results in following state space model

$$\begin{aligned} \mathbf{x}_{k+1}^m &= \begin{bmatrix} 0 & 1 \\ -0.5646 & 1.4920 \end{bmatrix} \mathbf{x}_k^m + \begin{bmatrix} 0 \\ 1 \end{bmatrix} v_k^{SP}, \\ v_k &= \begin{bmatrix} -0.262 & 0.0434 \end{bmatrix} \mathbf{x}_k^m. \end{aligned} \quad (34)$$

The pendulum model parameters were derived from time-domain identification method from system response to non-zero initial conditions leading to model (3) with parameters $\omega_n = 4.2167 \frac{rad}{s}$, $\xi = 0.0079$, $l = 0.552m$ and its discrete approximation (4).

The serial connection of both parts (motor and pendulum dynamics) then forms the total plant model G (6) which was used for the design of input shapers and the simulations. The command signal without any filtering and three different input shapers were used during the experiments. The time plots of the generated setpoint commands are shown in Fig. 4. Two filters were derived from finite horizon optimal control approach with and without positive cart acceleration constraint (21) respectively depending on whether we desire monotonous gantry velocity response or not. For the purpose of performance comparison with commonly used solutions, the standard Zero Vibration Derivative (ZVD) filter was implemented and the system was also excited by raw reference signal without any filtering.

The plots of data obtained from simulations with nominal plant realized in MATLAB-Simulink environment are displayed in Fig. 5. The curve colours correspond to Fig. 4 with the horizontal magenta dashed lines denoting the minimum and maximum limits of cart acceleration and jerk used as the constraints (19) in the optimization procedure ($a_{max} = 1 \frac{m}{s^2}$, $j_{max} = 40 \frac{m}{s^3}$). A minimum energy solution was found by setting $Q_i = 0$, $r_i = 1$ in the quadratic cost (23). First order flatness of residual vibration function was enforced from (12),(31) for $l = 1$ to improve robustness to modelling errors.

We can observe very good attenuation of oscillations when using all the considered command shapers compared to the case when no filter is used. At the same time, we can see that the acceleration and jerk constraints are precisely satisfied when using the optimal control approach but we have no

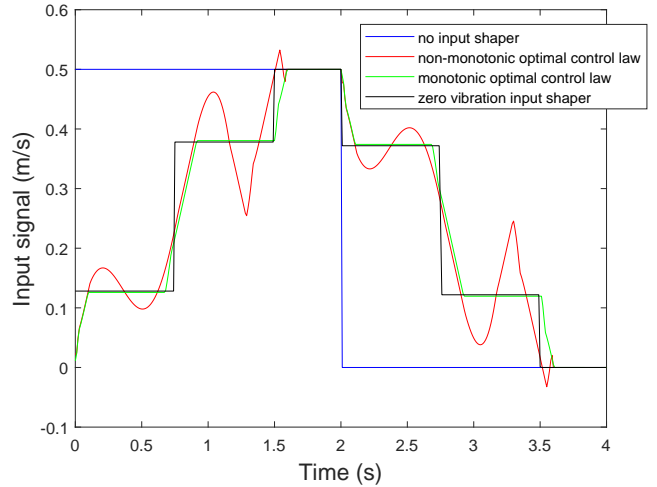


Fig. 4. Input signal

guarantee of meeting these limits when using the ZVD filter. The non-monotonous shaper achieves slightly faster settling times (approx. 0.2s) as shown in Fig. 5, exact finite-time transients are achieved for the whole plant.

The experimental results are given in Fig. 6. The plots are splitted into two parts by the vertical magenta dashed as proper time synchronization of the individual manoeuvres (i.e. acceleration and deceleration of the cart) was needed to directly compare different shapers. We can notice a slightly different behaviour of the real physical system compared to the simulations. This is mainly caused by unmodelled dynamics (mechanical friction, toothed belt dynamics). Nevertheless, the oscillation suppression is satisfactory for all the used shapers. The cart acceleration had to be computed by double differentiation from the measured cart position. A smoothed signal produced by zero-phase (non causal) Butterworth filter is shown to avoid excessive amplification of the quantization noise. It is seen that the acceleration limits are met almost exactly when using the optimal control sequence which is not the case of the trajectory generated by ZVD filter. The jerk measurement is not included as it is hard to be reconstructed from noisy position readings.

Fig. 7 shows the results after the previously described experiments were repeated on the physical system perturbed by shortening the pendulum length to half resulting in the change of natural frequency of the system. Degradation of performance is observed because of imperfect knowledge of the model parameters. The optimal shapers achieve similar level of robustness as the ZVD filter but generate smoother motion commands leading to physically feasible trajectories respecting the formulated actuator and plant limits.

VI. CONCLUSIONS

The paper presents a novel design method suitable for generation of optimal motion trajectories for human-operated gantry cranes. The proposed approach combines the quadratic optimization technique known from the field of MPC and

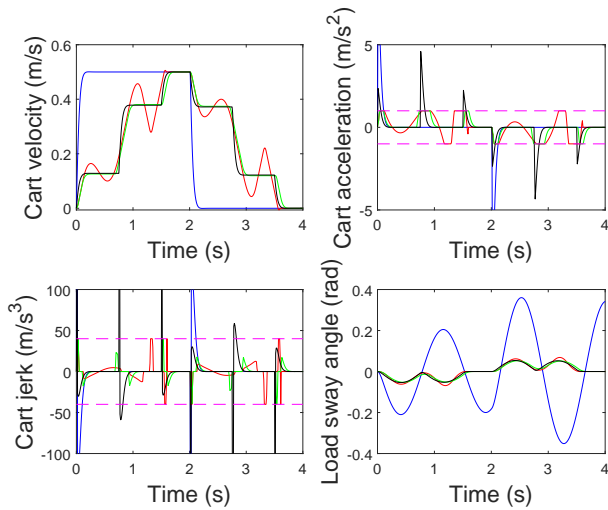


Fig. 5. Simulation results

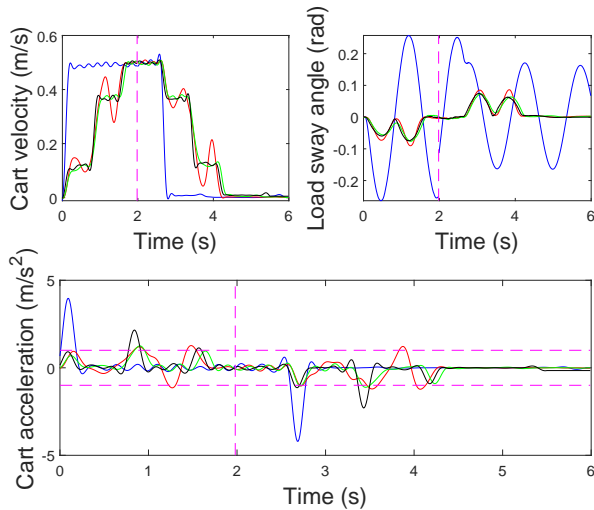


Fig. 6. Experiments with nominal plant

robust design methods used in the ZV input shaping. This allows to generate feasible motion trajectories reproducible by physical hardware while fully utilizing the available actuator resources. Optimal behavior can be achieved in various operating regimes by solving the design problem for different jog velocities and rope lengths. Finite-time transients are achieved for the whole plant, not only the part of the flexible dynamics. Specified level of robustness is imposed by shaping the residual vibration function. Future work will address the possibility of handling non-zero initial conditions, e.g. for rapid safe-stop movements, and multiple resonance modes of the system.

ACKNOWLEDGMENT

This work was supported from the H2020 ECSEL JU project I-MECH under grant agreement Nr. 737453 and from ERDF under project InteCom No. CZ.02.1.01/0.0/0.0/17_048/0007267.

REFERENCES

- [1] O. J. Smith, "Posicast control of damped oscillatory systems," *Proceedings of the IRE*, vol. 45, no. 9, pp. 1249–1255, 1957.

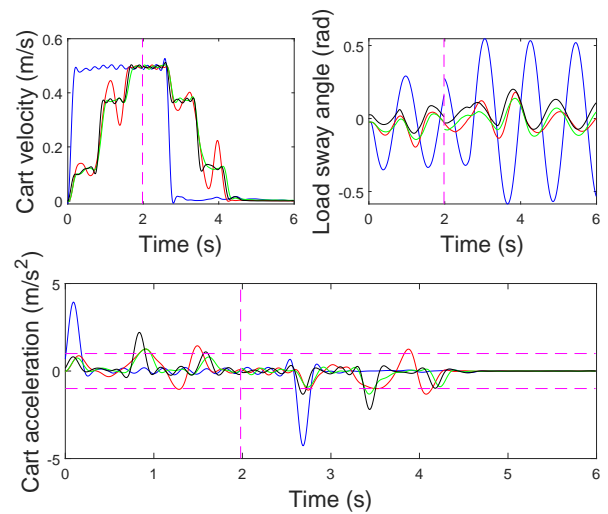


Fig. 7. Experiments with perturbed plant

- [2] N. C. Singer and W. P. Seering, "Using acausal shaping techniques to reduce robot vibration," in *Robotics and Automation, 1988. Proceedings., 1988 IEEE International Conference on*. IEEE, 1988, pp. 1434–1439.
- [3] N. C. Singer and W. Seering, "Preshaping command inputs to reduce system vibration," *Journal of Dynamic Systems, Measurement, and Control*, vol. 1027, pp. 1–23, 1990.
- [4] W. Singhose, W. Seering, and N. Singer, "Residual vibration reduction using vector diagrams to generate shaped inputs," *Journal of Mechanical Design*, vol. 116, no. 2, pp. 654–659, 1994.
- [5] T. Vyhřídál and M. Hromčík, "Parameterization of input shapers with delays of various distribution," *Automatica*, vol. 59, 2015.
- [6] M. O. T. Cole, "A class of low-pass FIR input shaping filter achieving exact residual vibration cancelation," *Automatica*, 2012.
- [7] B. Alikoç, T. Vyhřídál, and A. F. Ergenç, "Closed-form smoothers and shapers with distributed delay for damped oscillatory modes," *IET Control Theory Applications*, vol. 10, no. 18, pp. 2534–2542, 2016.
- [8] M. D. Baumgart and L. Y. Pao, "Discrete time-optimal command shaping," *Automatica*, vol. 43, no. 8, pp. 1403–1409, 2007.
- [9] J. Vaughan, A. Yano, and W. Singhose, "Comparison of robust input shapers," *Journal of Sound and Vibration*, vol. 315, no. 4, pp. 797–815, 2008.
- [10] M. Goubej and M. Schlegel, "Feature-based parametrization of input shaping filters with time delays," *IFAC Workshop on time delay systems, Prague*, 2010.
- [11] J. Vaughan, D. Kim, and W. Singhose, "Control of tower cranes with double-pendulum payload dynamics," *IEEE Transactions on Control Systems Technology*, vol. 18, no. 6, pp. 1345–1358, 2010.
- [12] W. Singhose, D. Kim, and M. Kenison, "Input shaping control of double-pendulum bridge crane oscillations," *Journal of Dynamic Systems, Measurement, and Control*, vol. 130, no. 3, p. 034504, 2008.
- [13] M. Giacomelli, F. Padula, L. Simoni, and A. Visioli, "Simplified input-output inversion control of a double pendulum overhead crane for residual oscillations reduction," *Mechatronics*, vol. 56, pp. 37–47, 2018.
- [14] M. Giacomelli, M. Faroni, D. Gorni, A. Marini, L. Simoni, and A. Visioli, "Model predictive control for operator-in-the-loop overhead cranes," in *2018 IEEE 23rd International Conference on Emerging Technologies and Factory Automation (ETFA)*, vol. 1, 2018, pp. 589–596.
- [15] N. Sun, Y. Wu, H. Chen, and Y. Fang, "An energy-optimal solution for transportation control of cranes with double pendulum dynamics: Design and experiments," *Mechanical Systems and Signal Processing*, vol. 102, pp. 87–101, 2018.
- [16] L. Ramli, Z. Mohamed, A. M. Abdullahi, H. Jaafar, and I. M. Lazim, "Control strategies for crane systems: A comprehensive review," *Mechanical Systems and Signal Processing*, vol. 95, pp. 1–23, 2017.
- [17] P. Balda, M. Schlegel, and M. Štětina, "Advanced control algorithms + simulink compatibility + real-time OS = REX," *16th IFAC World Congress*, 2006.